Letter

Magnetoelectricity induced by rippling of magnetic nanomembranes and wires

Carmine Ortix [1,*] and Jeroen van den Brink [2]

[1] *Dipartimento di Fisica "E. R. Caianiello," Universitá di Salerno, IT-84084 Fisciano (SA), Italy*

[2] *Institute for Theoretical Solid State Physics, IFW Dresden, Helmholtzstrasse 20, D-01069 Dresden, Germany*

(Received 2 September 2022; accepted 11 May 2023; published 23 June 2023)

Magnetoelectric crystals have the interesting property that they allow electric fields to induce magnetic polarizations, and vice versa, magnetic fields to generate ferroelectric polarizations. Having such a magnetoelectric coupling usually requires complex types of magnetic textures, e.g., of spiraling type. Here, we establish a previously unknown approach to generate linear magnetoelectric coupling in ferromagnetic insulators with intrinsic Dzyaloshinskii-Moriya interaction (DMI). We show that the effect of nanoscale curved geometries combined with the intrinsic DMI of the magnetic shell lead to a reorganization of the magnetic texture that spontaneously breaks inversion symmetry and thereby induces macroscopic magnetoelectric multipoles. Specifically, we prove that structural deformation in the form of controlled ripples activates a magnetoelectric monopole in the recently synthesized two-dimensional magnets. We also demonstrate that in zigzag-shaped ferromagnetic wires in planar architectures, a magnetic toroidal moment triggers direct linear magnetoelectric coupling.

DOI: 10.1103/PhysRevResearch.5.L022063

Two-dimensional (2D) atomic crystals can change their physical properties in response to external stimuli, such as strain, resulting in new effective materials. Electrons in graphene react to mechanical deformations as if electromagnetic fields were applied. Strain fields realize gauge fields that are opposite in the two valleys. These gauge fields lead to a complete reorganization of the electronic spectrum when they generate a "pseudomagnetic" field, i.e., a magnetic field opposite in the two valleys. The latter leads to pseudo-Landau levels [1] which have been imaged in graphene nanobubbles [2], and in flakes supported on nanopillars [3]. Strain-induced Landau levels have been also generated in triangular nanoprisms [4]. A periodic arrangement of pseudomagnetic fields with nanoscale periods and ensuing flat electronic minibands have been instead realized in buckled graphene superlattices [5].

A relevant question that arises is whether and how mechanical deformations change the magnetic properties of the recently synthesized 2D magnets [6–10]. The main point of this Letter is to show that in analogy with pseudo-Landau levels in graphene, magnetic 2D membranes react to mechanical deformations with a reorganization of the magnetic configuration that leads to a specific magnetoelectric multipole: the so-called magnetoelectric monopole [11]. Such a magnetic state reconfiguration results from the interplay between the local curvature of the structure and the magnetic order parameter [12–16]. The reorganization of the magnetic state we discuss here applies to 2D magnets with ferromagnetic arrangements and an out-of-plane magnetic easy axis, and is of special relevance for ferromagnetic insulators such as $CrBr_3$ [17,18], few-layer CrI_3 [7], and $Cr_2Ge_2Te_6$ [6]. The presence of a macroscopic magnetoelectric monopole moment yields a direct linear magnetoelectric coupling. This magnetoelectric capability based on a reorganization of the magnetic state is different in nature from the magnetoelectricity behavior predicted in ferromagnetic even-layer perovskites [19], which is induced by spin-dependent metal-ligand hybridization [20]. We also prove that zigzag-shaped magnetic wires in planar architectures undergo a magnetic state reorganization, which yields a different magnetoelectric multipole, a finite toroidal moment, with a magnetoelectric coupling that is linear as well be it of different symmetry.

We recall that magnetoelectric multipoles are defined by considering a spin system in an inhomogeneous magnetic field that varies slowly on the scale of the system size [21]. The interaction with the magnetic field gradient is then regulated by the tensor $\mathcal{M}_{ij} = \int \mathbf{r}_i \boldsymbol{\mu}_j(\mathbf{r}) d^3\mathbf{r}$, with $\boldsymbol{\mu}(\mathbf{r})$ the magnetization density. This can be decomposed into three irreducible tensors: the pseudoscalar $a = \mathrm{tr}\,\mathcal{M}_{ij}/3$ defining the magnetoelectric monopole [22]; the toroidal moment [23] dual to the antisymmetric part of the tensor $t_i = \epsilon_{ijk}\mathcal{M}_{jk}/2$; and the traceless symmetric tensor describing the quadrupole magnetic moment of the system. Being odd under both spatial and time-reversal symmetry, these three irreducible tensors yield a linear coupling between polarization $\mathbf{P}$ and magnetization $\mathbf{M}$. In particular, the two linear couplings $A\,\mathbf{P}\cdot\mathbf{M}$, A being the monopolization $A = a/V$, and $\mathbf{T}\cdot\mathbf{P}\times\mathbf{M}$ with $\mathbf{T} = \mathbf{t}/V$ representing the toroidization, are entirely symmetry allowed.

To establish how the magnetic ground state of a 2D magnet is affected by geometric deformations, we employ a continuum description that takes into account exchange,

*cortix@unisa.it

magnetocrystalline anisotropy (this accounts in a local approximation also for magnetostatic interactions), and an intrinsic Dzyaloshinskii-Moriya interaction (DMI) coupling. We take a form of DMI valid in material structures with $\mathcal{C}_{nv}$ symmetry [24], relevant for instance for Janus monolayers of CrI_3 [25] as well as for chromium tri-iodide monolayers on metal substrates [26] or electrically gated [27]. We consider the deformation to result in one-dimensional ripples with a geometry similar to that of graphene on $NbSe_2$ [5]. Even if such a buckled layer is locally flat, magnetomechanical geometric effects still come into play. Specifically, the confinement of the magnetic energy functional to the rippled surface results into an effective curvature-induced DMI coupling [28,29] originating from the exchange energy term, and an effective magnetic anisotropy controlled by the local curvature. The latter possesses two contributions of different nature (see Supplemental Material [30]). First, the intrinsic DMI interaction results in an effective anisotropy, which is of the easy-surface type or of the easy-normal (out-of-plane) type depending on the signed curvature (see Supplemental Material [30]). Second, there is an exchange-induced anisotropy that favors an alignment of the magnetic moments along the one-dimensional ripples. In magnetic shells with an easy-surface type of magnetocrystalline anisotropy, the magnetic ground state is set by this exchange-induced anisotropy (see Supplemental Material [30]). On the contrary, for magnetic layers with an out-of-plane ferromagnetic ground state [6,7] the exchange-induced DMI coupling is in full force and leads to inhomogeneous magnetic textures with the magnetic moments lying in the plane perpendicular to the ripples. Even more importantly, the presence of the DMI-induced anisotropy additionally alters the magnetic texture: It is this local change that triggers the appearance of magnetic multipole terms.

To show this, it is convenient to parametrize the direction of the normalized magnetization $\mathbf{m} = \mathbf{M}/M_s$, with M_s the saturated magnetization, in the locally flat reference frame [see Fig. 1(a)]. Since the magnetic moments lie in the plane perpendicular to the ripple, their direction can be determined introducing a local angle Θ that measures the canting of the moments away from the normal. Using that the period of the ripple λ is much larger than the exchange length l and the DMI length d, the canting angle obtained from the minimization of the magnetic energy functional can be expressed (see Supplemental Material [30]) as $\Theta \simeq -\kappa'(s)\, l^2/[1 + d\,\kappa(s)]$, where $\kappa(s)$ is the local curvature as a function of the arc length s in the corrugated direction, and all lengths have been measured in units of λ. Except for the points of maximum curvature, i.e., at the crests and valleys of the ripples, the canting angle is generally nonvanishing. The magnetic texture consequently acquires the periodicity of the corrugated structure. The crux of the story is that the intrinsic DMI coupling leads to a crest-valley asymmetry of the magnetic texture with an ensuing magnetically induced breaking of inversion symmetry.

Consider for instance regular periodic wrinkles with a simple sinusoidal shape. In the embedding three-dimensional Euclidean space [cf. Fig. 1(a)], this structure is centrosymmetric with the midpoints between the valleys and the crests corresponding to the inversion symmetry centers. Without

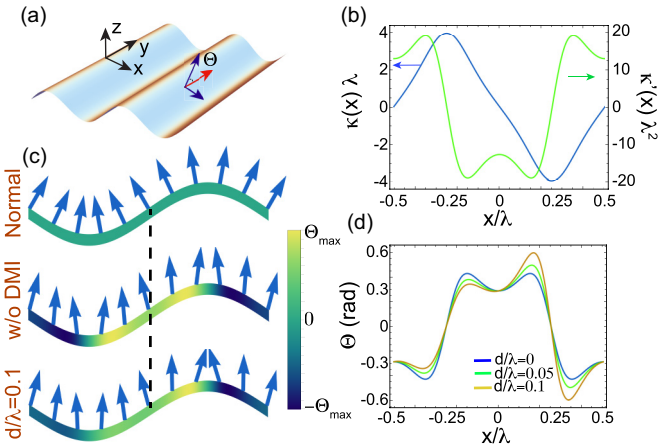

FIG. 1. (a) Sketch of a two-dimensional rippled surface with the Euclidean and the local curvilinear coordinates. Θ is the canting angle from the normal direction. (b) Behavior of the local curvature and of its first derivative for a ripple with a sinusoidal shape of height $h = 0.1\lambda$ as a function $\hat{x}$. (c) The magnetic ground state excluding curvature effects (top); with curvature effects but in the absence of an intrinsic DMI interaction (middle); and in the presence of DMI-induced curvature effects. The density plot shows the local canting angle along the rippled surface. (d) Behavior of the local canting angle of the magnetic texture in the absence ($d/\lambda = 0$) and presence ($d/\lambda = 0.05, 0.1$) of intrinsic DMI coupling. The exchange length $l/\lambda = 0.15$.

intrinsic DMI, the canting of the magnetic moments away from the normal direction, and hence the magnetic texture itself, is entirely set by the first derivative of the local curvature, which is even under inversion [cf. Figs. 1(b) and 1(c)]. Due to the oddness of the signed curvature, the DMI-induced effective anisotropy introduces a valley-crest asymmetry in the canting angle [cf. Figs. 1(c) and 1(d)], and inevitably breaks the inversion symmetry of the magnetic texture. This can be more easily shown by separating the compensated, i.e., with zero net magnetic moment, parts of the magnetic texture from the uncompensated ferromagnetic one that preserves the centrosymmetry of the corrugated layer. Figure 2(a) displays the zero-averaged magnetic texture decomposed in its two Euclidean components. The magnetic texture is inversion symmetric both when completely neglecting curvature effects, i.e., for $\Theta \equiv 0$, and when considering only exchanged-induced terms. In addition, it preserves the combined symmetry $\mathcal{M}_x\mathcal{T}$ where $\mathcal{T}$ indicates time-reversal symmetry while $\mathcal{M}_x$ is the vertical mirror operation with respect to the two mirror planes located at the crests and valleys of the wrinkle. A finite DMI breaks the centrosymmetry while still conserving $\mathcal{M}_x\mathcal{T}$. Note that $\mathcal{M}_x\mathcal{T}$ constrains the $\hat{z}$ and $\hat{x}$ components of the normalized magnetization to be respectively even and odd with respect to the mirrors located at $x = \pm\lambda/4$.

Having established that the intrinsic DMI coupling results in a magnetochiral state via its curvature-induced effective anisotropy, we next show that the end product of this phenomenon is the appearance of a nonvanishing magnetoelectric monopole moment [31]. We first recall that a main complication with the definition of higher-order magnetic moments

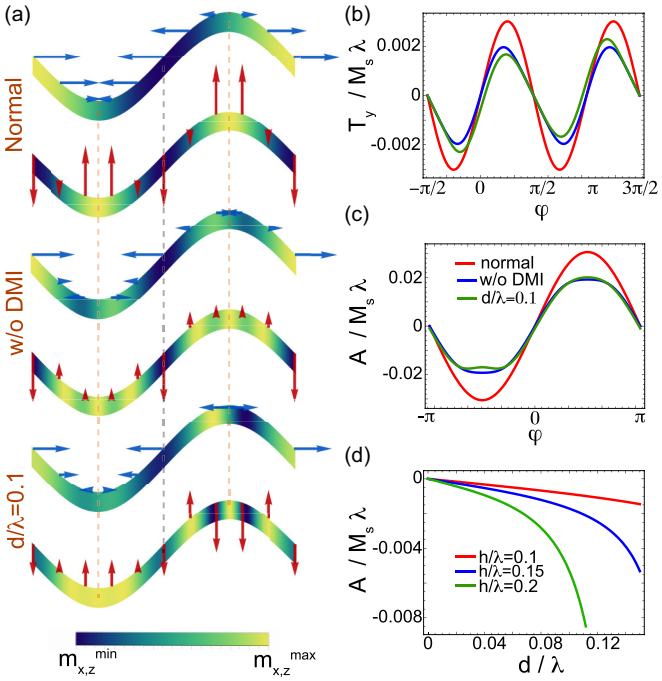

FIG. 2. (a) The $\hat{x}$ and $\hat{z}$ components of the compensated magnetic texture $\mathbf{m}(x) - \overline{m}$ by artificially neglecting curvature effects (top panels), including only exchange-induced curvature effects with $l/\lambda = 0.1$ (middle panels), and in the presence of the intrinsic DMI with $d/\lambda = l/\lambda$ (bottom panels). The ripple height $h = 0.1\lambda$. The gray dashed line indicates the inversion center of the ripple while the orange lines are the mirror points located at the crests and valleys of the ripple. The same for the phase dependence of the toroidization component T_y (b) and monopolization generated by the $\hat{x}$ component of the magnetization (c). The phase on the sinusoidal ripple profile has been imposed as $z(x) = h \sin(2\pi x/\lambda + \varphi)$. (d) Behavior of the total monopolization as a function of the intrinsic DMI length d/λ for ripples of different heights h. The exchange length has been set to $l/\lambda = 0.1$.

in periodic structures is the fact that, besides the origin dependence of uncompensated magnetic textures [11,23], they assume arbitrary values depending on the "unit cell" choice. This is analogous to the electric polarization in periodic crystals [32,33], which, according to the modern theory of polarization, can be only defined modulo a polarization quantum [34]. In atomic lattices, it has been suggested the existence of toroidization [23] and monopolization [11] quanta, with branch-independent changes in toroidization and monopolization that acquire physical meaning. The geometric superstructures of the present study are assumed to have periods order of magnitudes larger than the lattice constant. This makes the monopolization and toroidization lattices infinitely dense. Nevertheless, we can meaningfully define the magnetic moments in a continuum description using symmetry constraints. First, the uncompensated ferromagnetic $\hat{z}$ component $\overline{m} = \int \sqrt{g}\, m_z(x)dx / \int \sqrt{g}\, dx$, with $\sqrt{g}$ the line element of the ripple, preserves inversion symmetry. The related magnetoelectric multipoles do not have physical significance. Therefore, we only consider the contributions generated by the compensated magnetic texture. These are also subject to constraints imposed by (anti)unitary symmetries. Let us consider the $\hat{y}$ component of the toroidization measured in units of $M_s\lambda$ and defined by $T_y = \int \sqrt{g}\{z(x)m_x(x) - x[m_z(x) - \overline{m}]\}dx / \int 2\sqrt{g}dx$ where $z(x)$ indicates the local height of the ripple in the Monge gauge. To account for different choices of the supercell, we continuously sweep a phase φ on the sinusoidal ripple profile. Figure 2(b) displays the corresponding behavior of the toroidization. In the absence of intrinsic DMI ($d = 0$) the torodization has odd parity both around $\varphi = 0, \pi$, i.e., for unit cells centered at the inversion centers of the ripples, and around $\varphi = \pi/2, 3\pi/2$, in which case the unit cells are centered at the crests and valleys of the wrinkles. The presence of a finite intrinsic DMI removes the parity symmetry around $\varphi = 0, \pi$ but keeps the oddness around $\varphi = \pi/2, 3\pi/2$. This is because the phase dependence of the toroidization displays the same symmetries of the magnetic system, in analogy with the electric polarization lattice [11]. In particular, the odd parity around $\varphi = \pi/2, 3\pi/2$ results from the antiunitary $\mathcal{M}_x\mathcal{T}$ symmetry, which is conserved independent of the presence of the intrinsic DMI. Since $T_y \to -T_y$ under $\mathcal{M}_x\mathcal{T}$, we conclude that the macroscopic toroidization component T_y is forced to vanish. Analogously, also the $\hat{x}$ and $\hat{z}$ components of the macroscopic toroidization are vanishing due to the presence of the antiunitary $\mathcal{M}_y\mathcal{T}$ symmetry, which is preserved in the system since the magnetic moments are always orthogonal to the translationally invariant $\hat{y}$ direction.

With the macroscopic toroidization that is symmetry forbidden by the $\mathcal{M}_{x,y}\mathcal{T}$ symmetries, we next consider the magnetoelectric monopolization $A = \int \sqrt{g}\{x\, m_x(x) + z(x)[m_z(x) - \overline{m}]\}dx / \int 3\sqrt{g}dx$. In Fig. 2(c) we show the phase dependence of the monopolization associated with the $\hat{x}$ component of the compensated magnetic texture. It has odd parity around $\varphi = 0, \pi$ both when neglecting curvature effects all together and when accounting for exchange-induced terms. This signals the presence of inversion symmetry that is preserved as long as the intrinsic DMI coupling is neglected. With magnetic inversion symmetry breaking ($d \neq 0$) the phase dependence does not display any parity, thus implying a finite macroscopic monopolization. Its absolute value is uniquely determined by the fact that its zeroness with inversion symmetry fixes the "gauge" $\varphi \equiv 0, \pi$. Importantly, also the $\hat{z}$ component of the magnetic texture generates a finite monopolization. This, however, is phase independent for the simple reason that the monopolization local density is a periodic function. Figure 2(d) shows the total monopolization as a function of the intrinsic DMI length for ripples of different height h. Increasing curvature boosts the monopolization of a rippled two-dimensional ferromagnet. In the Supplemental Material [30], we show that in Janus $Cr(I, Br)_3$ monolayers with ripples of periodicity of tens of nanometers, the monopolization ranges in the $10^{-3}\,\mu_B/\text{Å}$ scale. Importantly, the bulk lithium transition metal phosphate $LiMnPO_4$ has been predicted [11] to host a similar net monopolization $A = 5 \times 10^{-3}\,\mu_B/\text{Å}^2$.

A free-energy expansion (see the Supplemental Material [30]) in the magnetization, electric polarization, and monopolization shows that this sizable monopolization leads to an electric polarization in the $\hat{z}$ direction at zero field, which changes linearly with an external magnetic field. Note that the order parameters in the Landau theory are homogeneous.

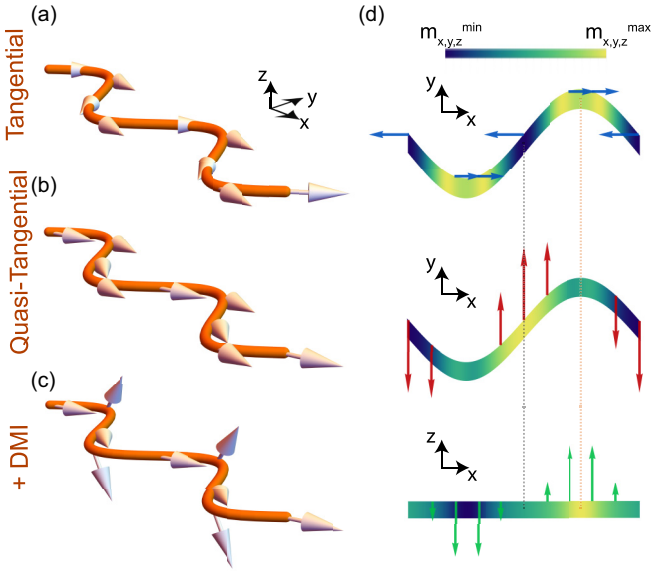

FIG. 3. (a)–(c) Tangential, quasitangential, i.e., including only exchange-induced curvature effects, and DMI-induced out-of-plane canted magnetic state for a zigzag magnetic nanowire. (d) shows the local behavior of the Euclidean components of the compensated normalized magnetic texture. We also show the inversion and rotation axis centers discussed in the main text.

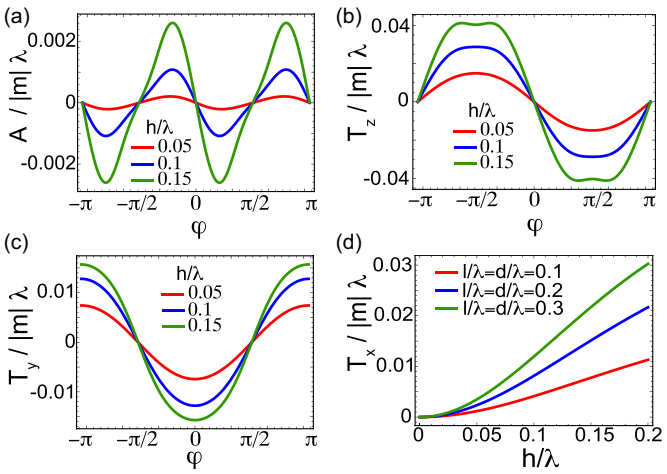

FIG. 4. (a)–(c) Phase dependence of the monopolization and toroidization components $T_{z,y}$ measured in units of $M_s\lambda$ with M_s the saturated magnetization. We have chosen $l/\lambda = d/\lambda = 0.1$. (d) Behavior of the toroidization as a function of the sinusoidal height h/λ.

The present mechanism is therefore distinguished from the inhomogeneous multiferroicity of spiral magnets [35] or due to dislocated spin-density waves [36,37].

We next show that magnetoelectric multipoles stabilized by the concomitant presence of geometric curvature and intrinsic DMI coupling can appear in zigzag-shaped magnetic wires in planar structures. In analogy with Refs. [38,39], we consider magnetic wires with a tangential anisotropy and a bulk DMI which applies to cubic noncentrosymmetric magnets of T and O symmetries [40]. We also take the DMI vector parallel to the tangential direction so that a straight wire has a magnetization parallel to it [see Fig. 3(a)]. In the absence of intrinsic DMI the magnetic state has a characteristic quasitangential distribution [38] [see Fig. 3(b) and the Supplemental Material [30]], uniquely identified by the azimuthal angle $\Phi \simeq \kappa'(s)\, l^2$. A finite intrinsic DMI yields a nonzero polar angle $\Theta \simeq \kappa(s)\, d/2$. Due to the intrinsic DMI-induced anisotropy, the magnetic textures then acquire a finite out-of-plane component [see Fig. 3(c)] whose period is set by the geometric curvature. This out-of-plane component yields a magnetically induced inversion symmetry breaking. To prove this, we assume the zigzag wire to have a sinusoidal shape. Figure 3(d) shows the corresponding compensated part of the magnetic texture decomposed into its three Euclidean components. Both the $\hat{x}$ and $\hat{y}$ components are even around the inversion centers $x = 0, \lambda$ due to the parity of the curvature derivative. Being related to the local curvature, the out-of-plane component has opposite parity and thus breaks inversion symmetry.

However, the complete magnetic state preserves two antiunitary symmetries. (i) The combined $\mathcal{C}_{2y}\mathcal{T}$ where $\mathcal{C}_{2y}$ is a twofold rotation with a $\hat{y}$-directed rotation axis intersecting the zigzag at its corners: This symmetry regulates the parity of the magnetic texture components (even for $m_{x,z}$ and odd for m_y) around the zigzag corners $x = \pm\lambda/4$. (ii) The combined $\mathcal{C}_{2z}\mathcal{T}$ where $\mathcal{C}_{2z}$ is the twofold rotation with an out-of-plane rotation axis intersecting the zigzag at the midpoints between the corners: This symmetry instead regulates the parity of the magnetic textures around $x = 0, \lambda/2$. These symmetries pose strong constraints on the presence of the macroscopic monopolization and toroidization. Consider first the monopolization whose phase dependence is shown in Fig. 4(a). Its odd parity around $\varphi = 0, \pi/2$ is consistent with the fact that both $\mathcal{C}_{2z}\mathcal{T}$ and $\mathcal{C}_{2y}\mathcal{T}$ send $A \to -A$. Consequently, the macroscopic monopolization is vanishing. Similarly, the odd parity of the toroidization component T_z around $\varphi = 0$ [see Fig. 4(b)] and that of T_y around $\varphi = \pi/2$ [see Fig. 4(c)] are the consequence of the presence of the $\mathcal{C}_{2z}\mathcal{T}$ and $\mathcal{C}_{2y}\mathcal{T}$ symmetry, respectively. Since $\mathcal{C}_{2y,z}\mathcal{T}$ send $T_{y,z} \to -T_{y,z}$ we conclude that a macroscopic toroidization, if present, has to be directed along the $\hat{x}$ direction. Figure 4(d) shows that the macroscopic torodization T_x is finite and increases monotonically, both increasing the profile amplitude h and the exchange and DMI length. Note that the macroscopic toroidization T_x does not display any phase dependence since its local density $\propto \sqrt{g}y(x)m_z$ is entirely periodic. Therefore, its absolute value can be defined without ambiguity.

Curvature effects in two-dimensional ferromagnetic insulators and magnetic wires thus result in magnetoelectric multipoles. This phenomenon stems from the interplay between the exchange-induced DMI and the intrinsic DMI-induced magnetic anisotropy which results in magnetically induced inversion symmetry breaking. This intramaterial magnetoelectricity is disjunct from the artificial magnetoelectric coupling [41,42] proposed in magnetic curved wires embedded in a piezoelectric matrix. Toroidal arrangements with ferrotoroidic domains have been shown to exist in the lithium transition metal phosphatate $LiCoPO_4$ [43]. Toroidization was also observed in an artificial crystals consisting of planar permalloy nanomagnets [44]. At the nanoscale, magnetoelectric multipoles have been suggested in insulating materials with magnetic skyrmions [45]. Our study

reveals that such multipoles can be designed at the nanoscale starting out even from a ferromagnetic ground state. The linear magnetoelectric coupling activated by monopolization and toroidization in these structures represent an important example of a geometry-induced effect at the nanoscale [46].

We thank D. Makarov, O. Pylypovskyi, K. Yershov, and P. Gentile for insightful discussions. C.O. acknowledges support from a VIDI grant (Project No. 680-47-543) financed by the Netherlands Organization for Scientific Research (NWO). This project was supported by the German Research Foundation (DFG) via the projects A05 of the Collaborative Research Center SFB 1143 (project-id 247310070) and through the Würzburg-Dresden Cluster of Excellence on Complexity and Topology in Quantum Matter ct.qmat (EXC 2147, Project No. 39085490).

[1] F. Guinea, M. I. Katsnelson, and A. K. Geim, Energy gaps and a zero-field quantum Hall effect in graphene by strain engineering, Nat. Phys. **6**, 30 (2010).

[2] N. Levy, S. A. Burke, K. L. Meaker, M. Panlasigui, A. Zettl, F. Guinea, A. H. C. Neto, and M. F. Crommie, Strain-induced pseudo–magnetic fields greater than 300 tesla in graphene nanobubbles, Science **329**, 544 (2010).

[3] Y. Jiang, J. Mao, J. Duan, X. Lai, K. Watanabe, T. Taniguchi, and E. Y. Andrei, Visualizing strain-induced pseudomagnetic fields in graphene through an hBn magnifying glass, Nano Lett. **17**, 2839 (2017).

[4] P. Nigge, A. C. Qu, E. Lantagne-Hurtubise, E. Mårsell, S. Link, G. Tom, M. Zonno, M. Michiardi, M. Schneider, S. Zhdanovich, G. Levy, U. Starke, C. Gutierrez, D. Bonn, S. A. Burke, M. Franz, and A. Damascelli, Room temperature strain-induced Landau levels in graphene on a wafer-scale platform, Sci. Adv. **5**, eaaw5593 (2019).

[5] J. Mao, S. P. Milovanović, M. Andelković, X. Lai, Y. Cao, K. Watanabe, T. Taniguchi, L. Covaci, F. M. Peeters, A. K. Geim, Y. Jiang, and E. Y. Andrei, Evidence of flat bands and correlated states in buckled graphene superlattices, Nature (London) **584**, 215 (2020).

[6] C. Gong, L. Li, Z. Li, H. Ji, A. Stern, Y. Xia, T. Cao, W. Bao, C. Wang, Y. Wang, Z. Q. Qiu, R. J. Cava, S. G. Louie, J. Xia, and X. Zhang, Discovery of intrinsic ferromagnetism in two-dimensional van der Waals crystals, Nature (London) **546**, 265 (2017).

[7] B. Huang, G. Clark, E. Navarro-Moratalla, D. R. Klein, R. Cheng, K. L. Seyler, D. Zhong, E. Schmidgall, M. A. McGuire, D. H. Cobden, W. Yao, D. Xiao, P. Jarillo-Herrero, and X. Xu, Layer-dependent ferromagnetism in a van der Waals crystal down to the monolayer limit, Nature (London) **546**, 270 (2017).

[8] N. Samarth, Magnetism in flatland, Nature (London) **546**, 216 (2017).

[9] K. S. Burch, D. Mandrus, and J.-G. Park, Magnetism in two-dimensional van der Waals materials, Nature (London) **563**, 47 (2018).

[10] M. Gibertini, M. Koperski, A. F. Morpurgo, and K. S. Novoselov, Magnetic 2D materials and heterostructures, Nat. Nanotechnol. **14**, 408 (2019).

[11] N. A. Spaldin, M. Fechner, E. Bousquet, A. Balatsky, and L. Nordström, Monopole-based formalism for the diagonal magnetoelectric response, Phys. Rev. B **88**, 094429 (2013).

[12] R. Streubel, P. Fischer, F. Kronast, V. P. Kravchuk, D. D. Sheka, Y. Gaididei, O. G. Schmidt, and D. Makarov, Magnetism in curved geometries, J. Phys. D **49**, 363001 (2016).

[13] D. D. Sheka, A perspective on curvilinear magnetism, Appl. Phys. Lett. **118**, 230502 (2021).

[14] D. Makarov, O. M. Volkov, A. Kákay, O. V. Pylypovskyi, B. Budinská, and O. V. Dobrovolskiy, New dimension in magnetism and superconductivity: 3D and curvilinear nanoarchitectures, Adv. Mater. **34**, 2101758 (2022).

[15] M. Yan, C. Andreas, A. Kakay, F. Garcia-Sanchez, and R. Hertel, Chiral symmetry breaking and pair-creation mediated Walker breakdown in magnetic nanotubes, Appl. Phys. Lett. **100**, 252401 (2012).

[16] A. Fernández-Pacheco, R. Streubel, O. Fruchart, R. Hertel, P. Fischer, and R. P. Cowburn, Three-dimensional nanomagnetism, Nat. Commun. **8**, 15756 (2017).

[17] D. Ghazaryan, M. T. Greenaway, Z. Wang, V. H. Guarochico-Moreira, I. J. Vera-Marun, J. Yin, Y. Liao, S. V. Morozov, O. Kristanovski, A. I. Lichtenstein, M. I. Katsnelson, F. Withers, A. Mishchenko, L. Eaves, A. K. Geim, K. S. Novoselov, and A. Misra, Magnon-assisted tunnelling in van der Waals heterostructures based on $CrBr_3$, Nat. Electron. **1**, 344 (2018).

[18] Z. Wang, I. Gutiérrez-Lezama, D. Dumcenco, N. Ubrig, T. Taniguchi, K. Watanabe, E. Giannini, M. Gibertini, and A. F. Morpurgo, Magnetization dependent tunneling conductance of ferromagnetic barriers, Nat. Commun. **12**, 6659 (2021).

[19] J. Zhang, Y. Zhou, F. Wang, X. Shen, J. Wang, and X. Lu, Coexistence and Coupling of Spin-Induced Ferroelectricity and Ferromagnetism in Perovskites, Phys. Rev. Lett. **129**, 117603 (2022).

[20] H. Murakawa, Y. Onose, S. Miyahara, N. Furukawa, and Y. Tokura, Ferroelectricity Induced by Spin-Dependent Metal-Ligand Hybridization in $Ba_2CoGe_2O_7$, Phys. Rev. Lett. **105**, 137202 (2010).

[21] N. A. Spaldin, M. Fiebig, and M. Mostovoy, The toroidal moment in condensed-matter physics and its relation to the magnetoelectric effect, J. Phys.: Condens. Matter **20**, 434203 (2008).

[22] As noted in Ref. [11], magnetic states with finite magnetoelectric monopoles do not imply a diverging **B** field. The divergence of the magnetization is compensated for by the divergence of the **H** field.

[23] C. Ederer and N. A. Spaldin, Towards a microscopic theory of toroidal moments in bulk periodic crystals, Phys. Rev. B **76**, 214404 (2007).

[24] H. Yang, A. Thiaville, S. Rohart, A. Fert, and M. Chshiev, Anatomy of Dzyaloshinskii-Moriya Interaction at Co/Pt Interfaces, Phys. Rev. Lett. **115**, 267210 (2015).

[25] C. Xu, J. Feng, S. Prokhorenko, Y. Nahas, H. Xiang, and L. Bellaiche, Topological spin texture in Janus monolayers of the chromium trihalides $Cr(I, X)_3$, Phys. Rev. B **101**, 060404(R) (2020).

[26] F. Zhang, X. Li, Y. Wu, X. Wang, J. Zhao, and W. Gao, Strong Dzyaloshinskii-Moriya interaction in monolayer CrI_3 on metal substrates, Phys. Rev. B **106**, L100407 (2022).

[27] J. Liu, M. Shi, J. Lu, and M. P. Anantram, Analysis of electrical-field-dependent Dzyaloshinskii-Moriya interaction and magnetocrystalline anisotropy in a two-dimensional ferromagnetic monolayer, Phys. Rev. B **97**, 054416 (2018).

[28] Y. Gaididei, V. P. Kravchuk, and D. D. Sheka, Curvature Effects in Thin Magnetic Shells, Phys. Rev. Lett. **112**, 257203 (2014).

[29] V. P. Kravchuk, U. K. Rößler, O. M. Volkov, D. D. Sheka, J. van den Brink, D. Makarov, H. Fuchs, H. Fangohr, and Y. Gaididei, Topologically stable magnetization states on a spherical shell: Curvature-stabilized skyrmions, Phys. Rev. B **94**, 144402 (2016).

[30] See Supplemental Material at http://link.aps.org/supplemental/10.1103/PhysRevResearch.5.L022063 for the details on the magnetic energy functional, the estimate of the magnetoelectric monopolization in Janus monolayers of chromium trihalides, and the multiferroic Landau theory.

[31] We note that magnetochirality is neither necessary nor sufficient for the occurrence of magnetoelectric multipole moments. Magnetic states with mirror symmetries can display a finite toroidal moment as exemplified by the case of a magnetic vortex on a square palette [21]. Combined antiunitary symmetries can instead force the multipoles of magnetochiral states to vanish.

[32] R. D. King-Smith and D. Vanderbilt, Theory of polarization of crystalline solids, Phys. Rev. B **47**, 1651 (1993).

[33] R. Resta, Macroscopic polarization in crystalline dielectrics: The geometric phase approach, Rev. Mod. Phys. **66**, 899 (1994).

[34] D. Vanderbilt and R. D. King-Smith, Electric polarization as a bulk quantity and its relation to surface charge, Phys. Rev. B **48**, 4442 (1993).

[35] M. Mostovoy, Ferroelectricity in Spiral Magnets, Phys. Rev. Lett. **96**, 067601 (2006).

[36] J. J. Betouras, G. Giovannetti, and J. van den Brink, Multiferroicity Induced by Dislocated Spin-Density Waves, Phys. Rev. Lett. **98**, 257602 (2007).

[37] The difference between the two mechanisms is also shown in the fact that helicoidal spin density waves [35] do not possess magnetoelectric multipoles.

[38] O. M. Volkov, D. D. Sheka, Y. Gaididei, V. P. Kravchuk, U. K. Rößler, J. Fassbender, and D. Makarov, Mesoscale Dzyaloshinskii-Moriya interaction: Geometrical tailoring of the magnetochirality, Sci. Rep. **8**, 866 (2018).

[39] D. D. Sheka, O. V. Pylypovskyi, O. M. Volkov, K. V. Yershov, V. P. Kravchuk, and D. Makarov, Fundamentals of curvilinear ferromagnetism: Statics and dynamics of geometrically curved wires and narrow ribbons, Small **18**, 2105219 (2022).

[40] D. Cortés-Ortuño and P. Landeros, Influence of the Dzyaloshinskii–Moriya interaction on the spin-wave spectra of thin films, J. Phys.: Condens. Matter **25**, 156001 (2013).

[41] O. M. Volkov, U. K. Rössler, J. Fassbender, and D. Makarov, Concept of artificial magnetoelectric materials via geometrically controlling curvilinear helimagnets, J. Phys. D **52**, 345001 (2019).

[42] D. D. Sheka, O. V. Pylypovskyi, P. Landeros, Y. Gaididei, A. Kákay, and D. Makarov, Nonlocal chiral symmetry breaking in curvilinear magnetic shells, Commun. Phys. **3**, 128 (2020).

[43] B. B. Van Aken, J.-P. Rivera, H. Schmid, and M. Fiebig, Observation of ferrotoroidic domains, Nature (London) **449**, 702 (2007).

[44] J. Lehmann, C. Donnelly, P. M. Derlet, L. J. Heyderman, and M. Fiebig, Poling of an artificial magneto-toroidal crystal, Nat. Nanotechnol. **14**, 141 (2019).

[45] S. Bhowal and N. A. Spaldin, Magnetoelectric Classification of Skyrmions, Phys. Rev. Lett. **128**, 227204 (2022).

[46] P. Gentile, M. Cuoco, O. M. Volkov, Z.-J. Ying, I. J. Vera-Marun, D. Makarov, and C. Ortix, Electronic materials with nanoscale curved geometries, Nat. Electron. **5**, 551 (2022).